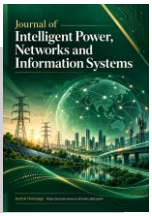
Journal of Intelligent Power, Networks and Information Systems

Journal Homepage: https://journal.unesa.ac.id/index.php/jipnis



Effect of Solar Irradiance Variation on Photovoltaic Power Output: A Single-Diode Simulation Study

1st Unit Three Kartini
Dept. Electrical Engineering
Universitas Negeri Surabaya
Surabaya, Indonesia
unitthree@unesa.ac.id

2nd Keisha Ghea Camalia
Dept. Electrical Engineering
Universitas Negeri Surabaya
Surabaya, Indonesia
kheisha.23105@mhs.unesa.ac.id

3rd Melani Aulia Elisa Putri
Dept. Electrical Engineering
Universitas Negeri Surabaya
Surabaya, Indonesia
melani.23130@mhs.unesa.ac.id

Abstract*— This study examines how controlled changes in solar irradiance affect the instantaneous electrical characteristics of a reference photovoltaic (PV) module using a reproducible single-diode simulation. Unlike resource-assessment studies that integrate solar irradiation across days or months, the analysis is restricted to current–voltage (I–V) behavior, power–voltage (P–V) characteristics, and the maximum power point (MPP) under constant cell temperature. A hypothetical 36-cell module is described by a photogenerated current of 8.70 A, reverse saturation current of 1.0×10^{-9} A, diode ideality factor of 1.35, series resistance of 0.28 Ω, and shunt resistance of 180 Ω. Irradiance is varied from 200 to 1000 W/m² at 25°C. Numerical solutions of the implicit diode equation yield the modeled short-circuit current, open-circuit voltage, fill factor, and maximum power at each operating point. The corresponding curves reveal that irradiance strongly controls current and MPP, whereas voltage changes more moderately. A linear power-scaling approximation is compared with the diode-model estimates, and a local ±20% perturbation around 600 W/m² is used to quantify sensitivity. All parameters are illustrative rather than derived from a commercial datasheet, and no experimental validation or real-weather analysis is claimed. The contribution is a transparent electrical-level benchmark that separates model-induced behavior from measured PV performance.

***Keywords*— photovoltaic module, solar irradiance, single-diode model, maximum power point, I–V characteristic, simulation**

I. INTRODUCTION

Photovoltaic conversion is governed by the instantaneous photon flux incident on a semiconductor junction and the internal electrical response of the module. Solar irradiance G (W/m²) is a power flux at a moment in time; solar irradiation H (kWh/m²) is its time integral. This distinction matters when a study concerns module output power rather than monthly energy yield. In a PV device, increased irradiance generally raises photogenerated current, but the effects on operating voltage, maximum-power voltage, and fill factor are determined by the nonlinear current–voltage characteristics [1]–[3].

A widely used representation of this response is the single-diode model (SDM), which balances light-generated current, diode recombination current, and losses associated with series and shunt resistance. The SDM has been employed to translate reference operating-condition parameters into output curves under different environments [2]–[5]. Its merit is a physically interpretable structure with relatively modest computational cost. The irradiance and temperature matrix specified by IEC 61853-1 further demonstrates why PV module rating cannot be inferred solely from a single standard test point [6].

Advanced models can account for spectral irradiance, complex temperature dynamics, heterogeneous module technologies, measured resistance changes, and experimentally calibrated parasitic parameters. However, a narrowly controlled simulation has a different purpose: it isolates a primary input and reveals the mechanisms embedded in a stated mathematical model. Previous research has emphasized that diode-model parameters are often not constant across irradiance and temperature [3], [4]. Therefore, a simulation using fixed illustrative values should be reported as a conditional benchmark, not as a demonstrated prediction for a particular manufactured module.

This work asks three focused questions. First, how do I–V and P–V curves change when irradiance varies from 200 to 1000 W/m² at a fixed cell temperature? Second, how much do maximum power and electrical characteristics depart from a simple proportionality-to-irradiance approximation? Third, how sensitive is output power to a controlled perturbation around a midrange operating point? These questions are intentionally distinct from an assessment of monthly global horizontal irradiation, seasonal resource variability, tilt-angle optimization, or annual energy yield. The study provides tabulated electrical outputs, reproducible equations, and figures accompanied by precise boundaries of interpretation.

II. MATERIALS AND METHODS

A. Photovoltaic Model and Working Assumptions

The PV module is represented by a current source Iph, one diode, a series resistance Rs, and a shunt resistance Rsh (Fig. 1). For module voltage V and current I, the governing equation is given by:

$$I = Iph - I0\{\exp[(V+IRs)/(nNskT/q) - \} - (V+IRs)/Rsh \quad (1)$$

In (1), I0 is diode reverse saturation current, n is the ideality factor, Ns is the number of series-connected cells, q is elementary charge, k is Boltzmann constant, and T is absolute cell temperature. This is an implicit relation because I appears on both sides. With T held at 298.15 K, irradiance

dependence is introduced solely through Iph(G) = Iph,ref (G/1000). The other electrical parameters remain constant by construction; this simplifying choice is not claimed to reproduce their real irradiance dependence.

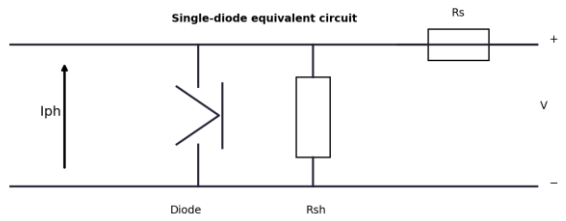


Fig. 1. Equivalent-circuit representation of the illustrative single-diode photovoltaic model.

TABLE I. REFERENCE MODEL PARAMETERS AND SIMULATION CONDITIONS

Parameter	Assumed value
Number of cells (Ns)	36 in series
Cell temperature (T)	25°C (298.15 K)
Reference irradiance	1000 W/m²
Photocurrent at reference	8.70 A
Reverse saturation current	1.0×10^{-9} A
Diode ideality factor	1.35
Series resistance (Rs)	0.28 Ω
Shunt resistance (Rsh)	180 Ω
Irradiance cases	200, 400, 600, 800, 1000 W/m²
Source of parameters	Declared hypothetical benchmark

The reference is not a named commercial module and the resulting standard-condition power is computed, rather than prescribed as a nominal nameplate rating. No weather file, instrument trace, historical resource series, or experimental calibration is introduced. This avoids treating synthetic electrical performance as measured field output.

B. Numerical Solution and Performance Metrics

For each prescribed irradiance, open-circuit voltage Voc is found from the I = 0 condition, and short-circuit current Isc from V = 0. The implicit current equation is solved by a bracketing root solver over 280 evenly spaced voltage samples between 0 and Voc; computed power follows P(V) = V I(V). The sampled maximum defines Pmp together with its corresponding Vmp and Imp. The fill factor is FF = Pmp/(Voc Isc). Numerical grid spacing and the bracketing tolerance (1×10^{-12} A for each current root) are specified so the calculation can be independently repeated.

A reference linear-scaling estimate is defined by Plin(G) = Pmp(1000) × (G/1000). The comparative departure is ΔP = [Pmp(G) − Plin(G)] / Plin(G) × 100%, with the 1000 W/m² case representing the common anchor. This departure should be interpreted as a difference between two mathematical models, not prediction error against physical measurements. No regression fit or hypothesis test is performed because all data points are deterministic numerical evaluations.

C. Irradiance Perturbation Design

A complementary scenario imposes irradiance changes of −20%, −10%, 0%, +10%, and +20% around G0 = 600 W/m², corresponding to 480, 540, 600, 660, and 720 W/m². The elasticity of output is approximated by finite differences, using normalized changes in Pmp divided by normalized changes in G around the baseline. Cell temperature and all diode parameters remain fixed. This isolates irradiance in the simplest possible manner and prevents the temperature-loss effects reserved for a separate thermal study from being silently incorporated here.

III. RESULTS AND DISCUSSION

A. Irradiance Effects on I-V Behavior

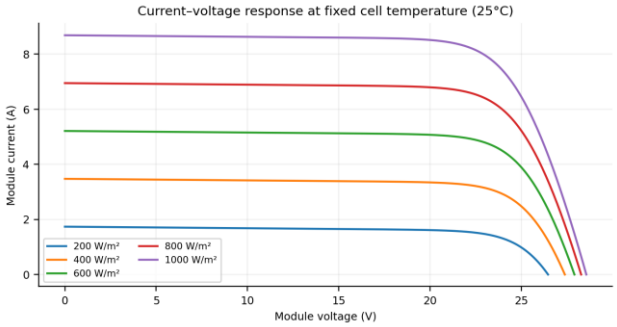


Fig. 2. Simulated current–voltage curves at five irradiance levels with cell temperature fixed at 25°C.

Figure 2 illustrates a family of I–V curves generated from the same electrical parameters. The increase in photocurrent causes the characteristic near-flat current region to shift upward as G increases. The curve knee also moves, indicating that the operating point delivering maximum power cannot be inferred from current scaling alone. The simulated voltage intercept varies by a smaller fraction than the current intercept: this is expected because the diode branch contributes a logarithmic irradiance dependence to Voc. Yet the quantitative values are conditional on the chosen ideality factor and saturation current [2], [3].

TABLE II. CALCULATED PHOTOVOLTAIC OUTPUT UNDER FIVE IRRADIANCE CONDITIONS

G (W/m²)	Isc (A)	Voc (V)	Vmp (V)	Pmp (W)	FF (%)
200	1.74	26.46	22.29	34.19	74.39
400	3.47	27.38	22.77	72.39	76.10
600	5.21	27.90	22.90	110.24	75.81
800	6.95	28.27	22.80	147.31	74.98
1000	8.69	28.55	22.72	183.42	73.95

Table II provides the complete working-point comparisons. Current is particularly useful as the directly irradiance-sensitive response, whereas Voc and Vmp reflect the coupled nonlinear terms. Although model outputs are calculated to high numerical precision, two-decimal reporting is more appropriate because the inputs themselves are illustrative and uncalibrated. The resulting precision should not be mistaken for confidence in real-module parameters.

B. Maximum-Power Behavior and Model Comparison

Figure 3 shows how increased irradiance raises the height of the P–V peak. The change is not equivalent to a pure vertical rescaling: the voltage coordinate of the maximum shifts because both diode current and resistive dissipation change as current rises. The maximum-power point can therefore be examined separately from the short-circuit current or open-circuit voltage.

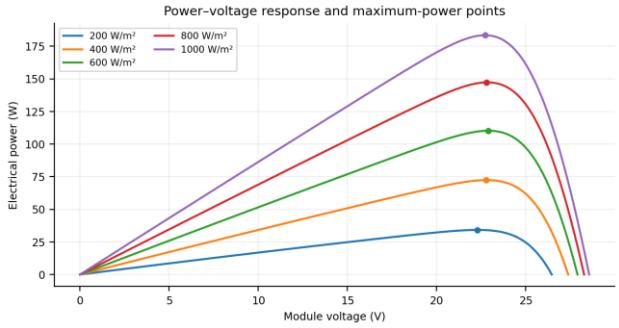


Fig. 3. Calculated P–V curves with simulated maximum-power points marked for each irradiance.

The model permits such separation without introducing a controller, inverter, or maximum-power-point-tracking algorithm, none of which is represented in this study.

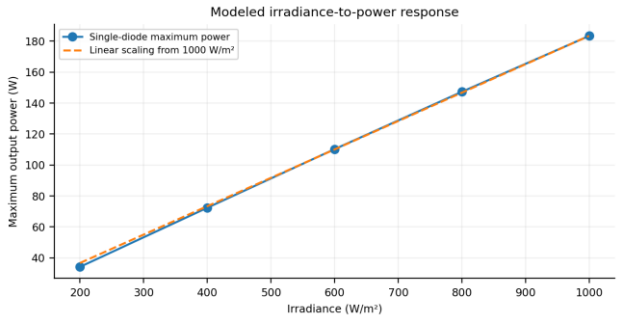


Fig. 4. Single-diode maximum power compared with proportional scaling anchored at 1000 W/m².

Figure 4 compares the model-derived peak power with a simple proportional rule. Differences between these curves quantify the electrical-model contribution beyond direct irradiance multiplication. Since reference parameters are held constant and module temperature is controlled, the comparison tests internal model structure, not real-world predictive superiority. In practical operation, temperature feedback, recombination, and irradiance-dependent parasitic losses can modify this relationship, as demonstrated by experimental parameter studies [3], [4].

C. *Local Sensitivity Around a Midrange Irradiance*

The sensitivity test in Table III and Fig. 5 reports the direct implications of changing irradiance around the 600 W/m² reference point. The percentage response can be compared with a one-for-one proportional increase.

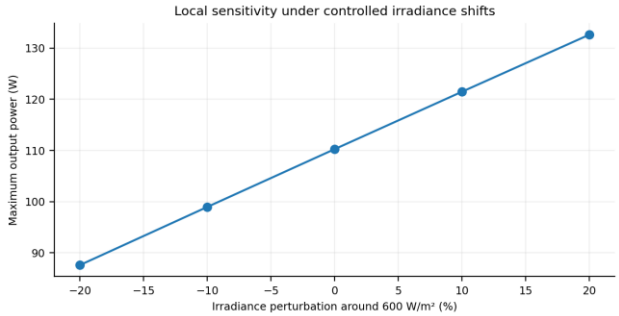


Fig. 5. Simulated maximum power in five prescribed sensitivity scenarios centered at 600 W/m².

TABLE III. LOCAL IRRADIANCE SENSITIVITY NEAR 600 W/m²

ΔG (%)	G (W/m²)	Pmp (W)	ΔPmp (%)
-20	480	87.60	-20.53
-10	540	98.95	-10.24
+0	600	110.24	+0.00
+10	660	121.45	+10.17
+20	720	132.59	+20.28

Deviations arise from the nonlinear equation and electrical resistive losses. This local design deliberately avoids annual yield integration or hypothetical climate trends; its purpose is to measure an electrical transfer relationship under controlled conditions. Because the table is generated from only five imposed input values, it contains no observational variance and cannot justify uncertainty intervals or claims of statistical significance.

D. *Technical Interpretation and Limitations*

Three implications follow from the numerical experiment. First, the module current response changes markedly over the irradiance range, so fixed-current assumptions can distort operating-point estimates. Second, the movement of the P–V knee means that output changes are not fully explained by a single scalar irradiance multiplier. Third, the extent and even direction of departure from a linear power approximation depends on assumed electrical parameters; a comparison across actual products requires data-sheet identification and parameter extraction [2], [5]. Accordingly, no universal numerical conversion coefficient is proposed.

The model has several deliberate constraints. Cell temperature is constant at 25°C, although real panels can heat under increasing irradiance. The module is spatially uniform and unshaded; bifacial gain, series mismatch, spectral content, and converter operation are excluded. The series/shunt resistances and reverse saturation current are held fixed across all cases, whereas experimental studies have shown dependencies that can become important at low light [3], [4]. The voltage grid introduces a small discretization error in Pmp; tighter sampling or scalar optimization could further refine the numerical maximum if required.

The present article differs in its outcome variable and interpretation from an irradiation resource simulation: the first is concerned with energy integrated over time, while this study solves a nonlinear module equation to obtain instantaneous power and electrical parameters. It also does not estimate thermal performance, tilt optimization, daily yield dynamics, or joint environmental effects, thereby retaining a clearly bounded analytical contribution. A natural next step is to calibrate the hypothetical module against a real manufacturer datasheet and compare simulated I–V curves with a controlled solar simulator, following irradiance–temperature test matrices such as IEC 61853-1 [6]. Such external validation is explicitly outside the available evidence.

IV. CONCLUSION

A reproducible single-diode simulation was used to isolate the effect of solar irradiance on instantaneous photovoltaic output across 200–1000 W/m² while maintaining module temperature at 25°C. The modeled I–V and P–V curves demonstrate an increasing photogenerated current, a more moderate voltage response, and a moving

maximum-power point as irradiance changes. Numerical tables describe the open-circuit and short-circuit conditions, fill factor, and maximum power for each scenario. Linear scaling and local perturbation comparisons show which departures are introduced by the model's diode and resistance terms rather than by an assumed external dataset.

The results are synthetic and conditional on declared, uncalibrated module parameters. They do not constitute measured efficiencies, manufacturer ratings, experimental validation, or predictions of annual energy production. Their value lies in a transparent and technically interpretable electrical response benchmark that can support future calibration studies. Future work should estimate module-specific single-diode parameters, examine parameter variation under irradiance and cell temperature, and validate I–V predictions against measured current–voltage sweeps.

A. Numerical Consistency and Interpretation of Model Outputs

A reproducible model requires explicit verification beyond attractive plots. In every irradiance case, the calculated current at a prescribed voltage was obtained by solving the full implicit balance rather than treating a diode equation as an explicit relation. The terminal-current root is bracketed, which avoids dependence on an arbitrary Newton–Raphson initial guess. Open-circuit voltages are computed independently by setting terminal current equal to zero, and each current–voltage trace is evaluated only on the corresponding interval from zero to the appropriate open-circuit voltage. Because the diode current grows steeply as terminal voltage approaches open circuit, a common voltage interval for all curves would otherwise include nonphysical or negative-current operating points.

The maximum-power estimate in this implementation is the maximum of a 280-point discretization of the power–voltage curve. This makes the tabulated value a numerical approximation to the mathematical maximum. A denser grid or bounded scalar maximization may shift the final decimal digits of maximum-power voltage and power, but should not reverse the general curve ordering. In a later calibration exercise, convergence should be quantified as the change in Pmp when the voltage grid is doubled, rather than presuming that reported decimal places signify engineering accuracy. The exact solution of the terminal-current root and the discretized search for maximum power are distinct numerical operations and should not be confused.

An additional consistency constraint is that the calculated fill factor must remain dimensionless and below unity for this passive model. It is also essential to keep volts, amperes, ohms, kelvin, and W/m² internally consistent. The thermal-voltage factor is determined at the individual-cell scale and multiplied by the number of series cells in the module. Omitting the series-cell factor would yield an incorrectly sharp diode response and a materially different open-circuit voltage. The reference irradiance of 1000 W/m² enters only through the photocurrent scaling law; it is not itself an energy quantity, and no hours or annual production factors appear anywhere in the calculation.

The comparison with linear scaling should not be interpreted as a comparison between a sophisticated calibrated simulator and a measured baseline. Both approaches are analytical constructs based on assumptions; the linear baseline uses the 1000 W/m² model result as its anchor, while the single-diode curve introduces additional behavior through its voltage-dependent diode and resistance terms. Their divergence illustrates why different approximation levels need to be distinguished, but cannot establish predictive advantage without independent measurements. This is particularly relevant when designing low-cost PV teaching experiments, for which a transparent parameter record may be more useful than a black-box energy number.

Interpretation should also distinguish maximum available electrical power from power delivered to a connected load. The curves show a theoretical MPP of the module at each prescribed irradiance. A fixed resistive load, a battery-charging circuit, or an inverter without successful maximum-power-point tracking may operate away from the peak, in which case delivered power is smaller. The simulation makes no claim about control losses, load matching, DC–DC conversion, or inverter efficiency. These exclusions are necessary to ensure that the reported dependent variable remains the intrinsic module-level Pmp defined by the circuit model.

B. Implications for Future PV Experiments

For an empirical follow-up, a real module should first be identified with a traceable datasheet, including open-circuit voltage, short-circuit current, maximum-power voltage, maximum-power current, temperature coefficients, and the standard test condition. Parameters can then be extracted from the datasheet or fitted to measured I–V traces. Outdoor tests should record in-plane irradiance and cell or backsheet temperature simultaneously with electrical traces; measurements taken at mismatched times cannot isolate irradiance effects. Repeated sweeps across irradiance bands would support an assessment of measurement repeatability and model prediction error, which this deterministic study does not provide.

The electrical analysis could be extended in two directions while retaining a clear scientific question. One direction is a calibrated comparison of alternative single-diode parameter-translation equations across irradiance levels. Another is an experiment showing how accurately a compact electrical model estimates the maximum power of one identified module under controlled light intensities. Neither requires large numbers of unrelated graphs; instead, each requires a well-chosen benchmark, explicit loss function, and a quantitative comparison between predicted and observed operating points. In both designs, the inferred accuracy would be conditional on the instrument calibration, reference-device spectral match, and temperature measurement procedure [6].

REFERENCES

[1] PV Performance Modeling Collaborative, "Modeling guide." [Online]. Available: https://pvpmc.sandia.gov/modeling-guide/ (accessed Oct. 26, 2026).

[2] W. De Soto, S. A. Klein, and W. A. Beckman, "Improvement and validation of a model for photovoltaic array performance," Solar Energy, vol. 80, no. 1, pp. 78–88, 2006, doi: 10.1016/j.solener.2005.06.010.

[3] C. S. Ruschel, F. P. Gasparin, and A. Krenzinger, "Experimental analysis of the single diode model parameters dependence on irradiance and temperature," Solar Energy, vol. 217, pp. 134–144, 2021, doi: 10.1016/j.solener.2021.01.067.

[4] “Variations of PV module parameters with irradiance and temperature,” Energy Procedia, vol. 134, pp. 276–285, 2017, doi: 10.1016/j.egypro.2017.09.617.

[5] M. T. Boyd and C. Hansen, “Single diode equivalent circuit models,” PV Performance Modeling Collaborative, NIST, 2013. [Online]. Available: https://www.nist.gov/publications/single-diode-equivalent-circuit-models.

[6] IEC 61853-1:2011, “Photovoltaic (PV) module performance testing and energy rating—Part 1: Irradiance and temperature performance measurements and power rating,” International Electrotechnical Commission, 2011.

[7] PV Performance Modeling Collaborative, “PVsyst module model.” [Online]. Available: https://pvpmc.sandia.gov/modeling-guide/2-dc-module-iv/single-diode-equivalent-circuit-models/pvsyst-module-model/.

[8] “A novel one-diode model for enhanced performance modelling of photovoltaic systems,” Renewable Energy, vol. 264, Art. no. 125542, 2026, doi: 10.1016/j.renene.2026.125542.

[9] “Environmental-data-driven reconstruction of photovoltaic single-diode model parameters from irradiance and temperature measurements,” Energies, vol. 19, no. 17, Art. no. 3957, 2026. [Online]. Available: https://www.mdpi.com/1996-1073/19/17/3957.